

1
2
3
4

SEISMIC PERFORMANCE AND MODELING OF POST-TENSIONED, PRECAST CONCRETE SHEAR WALLS

1
2
3
4

Ahmet Can Tanyeri, Department of Civil and Environmental Engineering, University of California, Berkeley, CA

Jack P. Moehle, PhD, PE, Department of Civil and Environmental Engineering, University of California, Berkeley, CA

Takuya Nagae, PhD, National Research Institute for Earth Science and Disaster Prevention, Japan

1
2

ABSTRACT

1
2
3
4
5
6
7
8
9
10
11
12
13
14
15
16
17
18
19
20
21
22
23
24
25
26
27
28
29
30
31
32
33
34
35
36
37
38
39
40
41
42
43
44
45
46
47
48
49
50
51
52
53
54
55
56
57
58
59
60
61
62
63
64
65
66
67
68
69
70
71
72
73
74
75
76
77
78
79
80
81
82
83
84
85
86
87
88
89
90
91
92
93
94
95
96
97
98
99
100

In December 2010, the National Research Institute for Earth Science and Disaster Prevention (NIED) in Japan conducted a three-dimensional earthquake simulation test on a full-scale, four-story building using the E-Defense shaking table. The seismic force-resisting system of the test building comprised two post-tensioned (PT) frames in one direction and two unbonded PT precast walls in the other direction. The building was designed using the latest code requirements and design recommendations available both in Japan and the U.S., including the ACI ITG-5.2-09¹. The test building was subjected to several earthquake ground motions, ranging from serviceability level to near collapse.

This study aims to develop practical structural engineering models that are capable of simulating the important response characteristics of the building subjected to moderate to extreme earthquake shaking. The results of the tests and the analytical simulations provide an opportunity to better understand the response characteristics of PT walls and assess the ability of nonlinear analytical models to simulate important global and local responses, including three-dimensional system interactions, both prior to and after loss of significant lateral strength.

1
2

Keywords: Earthquake simulation test, Shear wall, Precast concrete, Unbonded post-tensioning, Nonlinear dynamic analysis

INTRODUCTION

Past earthquakes have shown examples of unsatisfactory performance of buildings using reinforced concrete structural walls as the primary lateral force-resisting system. In the 1994 Northridge earthquake examples can be found where walls possessed too much overstrength, leading to unintended failure of collectors and floor systems, including precast and post-tensioned construction. In the 2010 Chile and 2011 Christchurch earthquakes, many structural wall buildings sustained severe damage. Although some differences in detailing practices exist between those countries and the U.S., the failure patterns raise concerns about how well conventionally reinforced structural walls in U.S. buildings will perform during the next earthquake. Past research efforts, including the PREcast Seismic Structural Systems (PRESS) program² and subsequent studies, have explored alternative design approaches using post-tensioned (PT) precast structural walls to better control yielding mechanisms and promote self-centering behavior. These studies have provided excellent guidance on design and construction requirements, but examples of full-scale, three-dimensional dynamic tests to demonstrate behavior in realistic structural systems have been lacking. Such demonstrations are important to identify complex interactions that occur in complete building structures. Such demonstrations also are useful to serve as a vehicle for acceptance by the engineering community.

In December 2010, the National Research Institute for Earth Science and Disaster Prevention (NIED) in Japan conducted a three-dimensional earthquake simulation test on a full-scale, four-story building using the E-Defense shaking table (Figure 1). Design, instrumentation, preliminary numerical studies, and testing of the building were a collaboration among researchers from Japan and the U.S. The seismic force-resisting system of the test building comprised two bonded PT frames in one direction and two unbonded PT precast walls in the other direction. The building was designed using the latest code requirements and design recommendations available both in Japan and the U.S., including ACI ITG-5.2-09¹. The test building was subjected to several earthquake ground motions, ranging from serviceability level to near collapse.

Three-dimensional earthquake simulation testing of full-scale specimens is rare. Data from this test give a unique opportunity to understand the behavior of the unbonded PT walls and their interaction with other structural elements during an earthquake. In this study, the authors developed practical structural engineering models for the wall direction of the building. A comparison of the simulation and test results is done to assess the capability of currently available models to simulate the response of a real PT building under gradually increasing earthquakes.



Fig. 1 Picture of the Specimen

OVERVIEW OF THE TEST

TEST SPECIMEN

The test specimen was a full-scale, four-story, post-tensioned precast concrete building. It had a rectangular plan (Figure 2), with dimensions 7.2 m in the Y (transverse) direction and 14.4 m in the X (longitudinal) direction. Height of each floor was 3 m, resulting in total building height of 12 m. The lateral-load-resisting system in the Y direction was two precast unbonded PT shear walls and one bay unbonded PT center frame at B Axis. In the X direction the structural system consisted of two-bay bonded PT frames. All the structural elements were precast off-site and installed and post-tensioned on-site. Post-tensioning tendons of beams and columns in the X direction were bonded with grouting after installation. On the other hand, PT tendons of shear walls and beams in the Y direction were constructed to be unbonded from concrete.

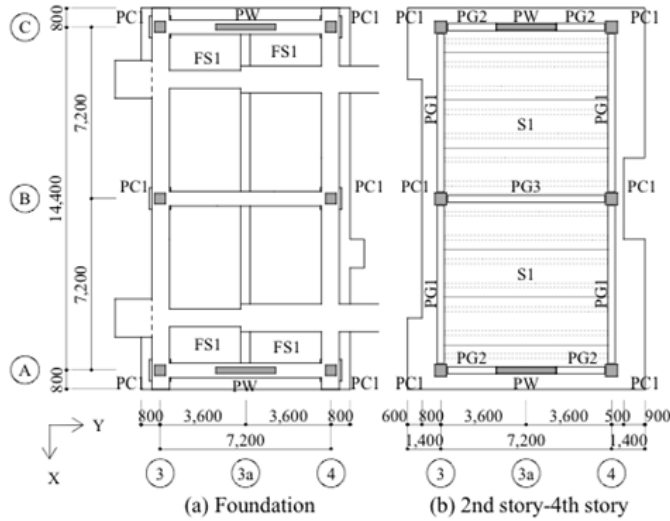


Fig. 2 Plan View of the Specimen (Unit: mm)

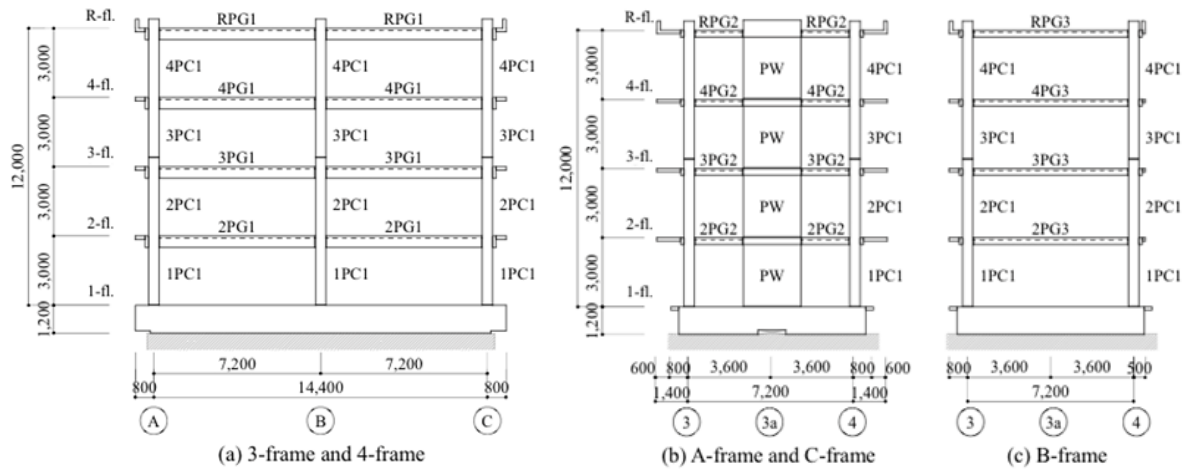


Fig. 3 Elevation View of the Specimen (Unit: mm)

Shear walls had a rectangular cross section with a length of 2500 mm and a thickness of 250 mm. PT walls were 12 m high, and therefore had a slenderness ratio of $H_w/l_w = 4.8$. Columns (PC1) had 450-mm square cross sections. Beams (PG2 & PG3) were partially precast, with the top 100 mm of the 300 mm by 300 mm section cast in place with the slab. The slab was 130 mm thick with the top 100 mm cast in place monolithically with the beams. The slab was supported by pretensioned joists with 1 m interval in the transverse direction. See Table 1 for additional details³.

Concrete design strength was 60 MPa for precast parts and 30 MPa for cast-in-place parts. The design strength of the grout mortar was 60 MPa. The first two floors of the north wall were constructed using FRCC (fiber reinforced cement composite). Nominal strength of the generic steel bar was 345 MPa. Transverse reinforcement of beams and walls in the Y direction was high strength steel bars with nominal strength of 785 MPa. Although columns were designed for required shear reinforcement by the Japanese Building Standard Law, the column core was not intentionally confined. PT rods of the columns were high strength steel

with 1080 MPa design strength. PT strands used in walls and beams had design strength of 1600 MPa. Test results of the materials are shown in Table 3.

Reinforcement details of the PT walls and wall-to-beam joint details are shown in Figure 4. Eight D22 (22 mm diameter) steel energy dissipation bars were unbonded through the lower 1.5 m of the first story and connected to the foundation with mechanical couplers. Effective prestressing of the PT tendons was 0.6 times the yield strength for the walls and PG2 beams, and 0.8 times the yield strength for the other beams and columns.

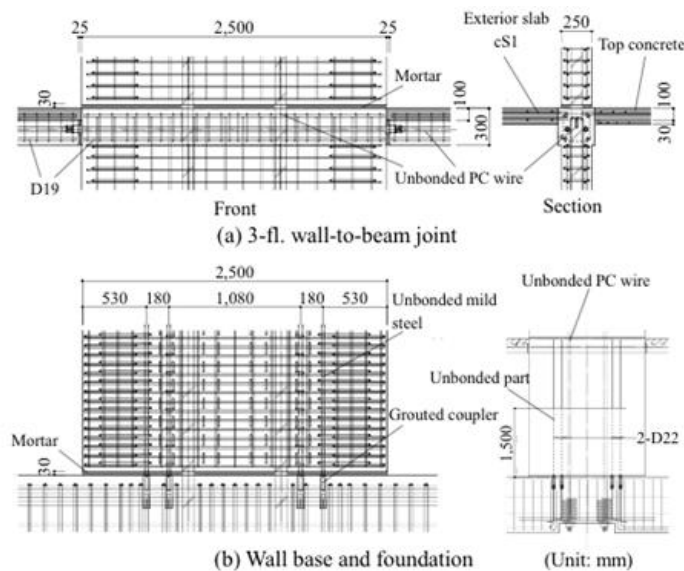


Fig. 4 Reinforcement Details of Walls (Unit: mm)

The total weight of the specimen was 5592 kN. The weight of each floor was 996 kN for Roof, 813 kN for 3rd floor, 806 kN for 2nd floor, and 804 kN for the 1st floor.

Table 1 Member Cross-Sections

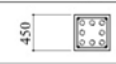
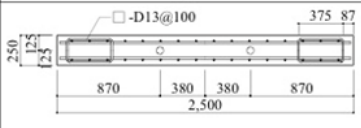
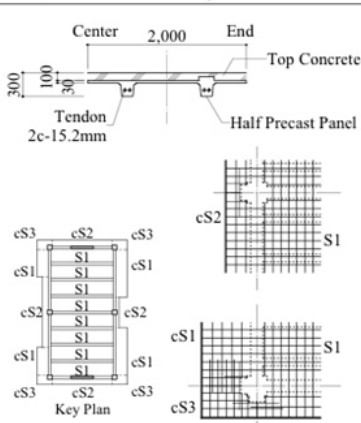
List of Column			List of Girder			List of Wall			
All	Section		R-fl.	Location	End	Center	4-fl.	Section	
	Tendon	8-21mm(SBPR1080/1230)		Tendon	4C-1-17.8mm(SWPR19L)	Tendon			3-10-15.2mm(SWPR7B)
	Rebar	4-D19		Top	2 - D19	V bar			D13@150(double)
	Hoop	D10@100		Bottom	3 - D19	H bar			D13@100(double)
List of Slab Depth: 130mm			4-fl.			3-fl.			
			Section			Top Section			
			Tendon			Bottom Section			
			Top			Tendon			
			Bottom			Top			
			Stirrup			Bottom			
			3-fl.			2-fl.			
			Section			Section			
			Tendon			Tendon			
			Top			Top			
			Bottom			Bottom			
			Stirrup			Stirrup			
			2-fl.			1-fl.			
			Section			Section			
			Tendon			Tendon			
			Top			Top			
			Bottom			Bottom			
			Stirrup			Stirrup			
			Key Plan						
			List of Girder			List of Wall			
			PG2			PG3			
			Section			Section			
			Tendon			Tendon			
			Top			Top			
			Bottom			Bottom			
			Stirrup			Stirrup			
			Shorter direction			Longer direction			
			S1			S1			
			cS1			cS1			
			cS2			cS2			
			cS3			cS3			
			Top			Top			
			Bottom			Bottom			
			Top			Top			
			Bottom			Bottom			
			Top			Top			
			Bottom			Bottom			

Table 2 Effective prestress and permanent axial load

	P_e [kN]	N_L [kN]
1PC1 (B-axis)	2274	733
1PW	2666	176
2PG1	1822	-
2PG2	338	-
2PG3	338	-

(Unit: mm)

Table 3 Material Test Results

(a) Concrete		(b) Grout	
	σ_B [N/mm ²]		σ_B [N/mm ²]
PCa	83.2	Mortar	135.6
PCa (F)	85.5	Mortar (F)	120.3
Top	40.9	Milk cement	63.4

(c) Steel		
	σ_y [N/mm ²]	σ_t [N/mm ²]
PC bar ϕ 21 (Column, SBPR1080/1230)	1194	1277
D22 (Wall, SD345)	385	563
D19 (Column and beam, SD345)	389	561
D13 (Wall, SD295A)	347	501
D13 (Slab, SD295A)	372	522
D10 (Column and beam, SD295A)	361	518
D10 (Slab, SD295A)	388	513
D13 (Wall and PG2, KSS785)	938	1107
	F_y [kN]	F_t [kN]
PC wire ϕ 15.2 (Wall, SWPR7BL)	250	277
PC wire ϕ 15.2 (Beam, SWPR7BL)	255	279
PC wire ϕ 17.8 (Beam, SWPR19L)	356	404
PC wire ϕ 19.3 (Beam, SWPR7BL)	429	481

INPUT MOTIONS

Input ground motions were scaled JMA-Kobe and JR-Takatori records from 1995 Kobe earthquake. The motions were applied in two horizontal and vertical directions simultaneously. Firstly, JMA-Kobe motion was applied with wave amplitude scale factor of 10%, 25%, 50%, and 100%, respectively. Lastly, 40% and 60% JR-Takatori were applied. This paper considers the 25%, 50% and 100% excitations only. Figure 5 shows time records and acceleration response spectra of input motions.

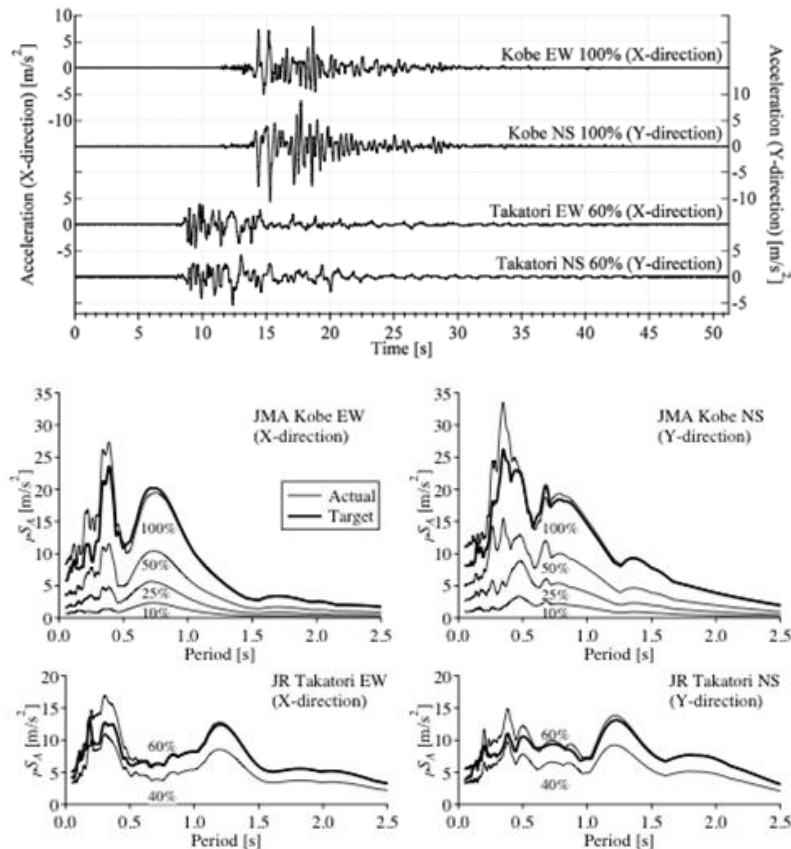


Fig. 5 Time Records and Acceleration Response Spectra of the Input Motions

NUMERICAL SIMULATION

A three-dimensional numerical model of the Y direction of the specimen was implemented using the computer program Perform 3D⁴. Figures 6 & 7 show 3D and elevation view of the computer model.

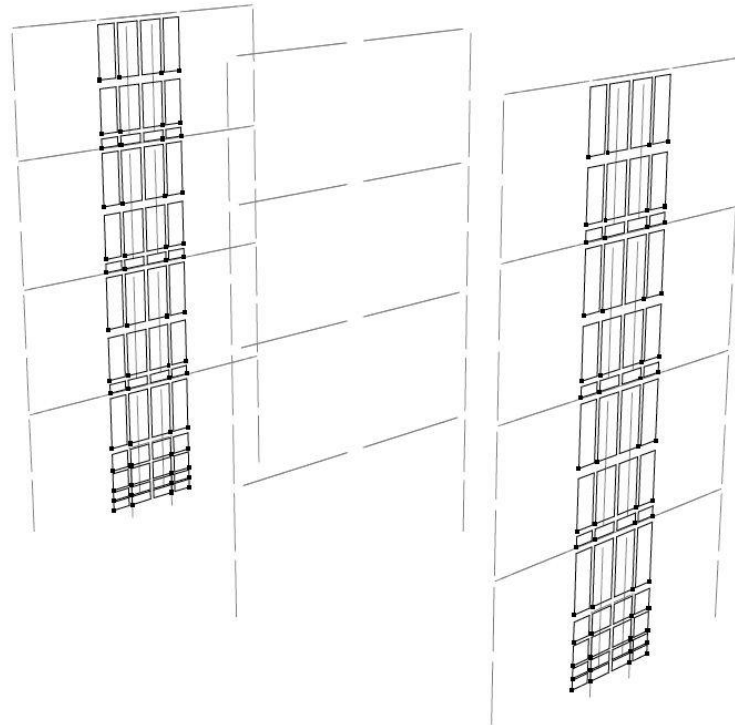


Fig. 6 3D View of the Perform 3D Model

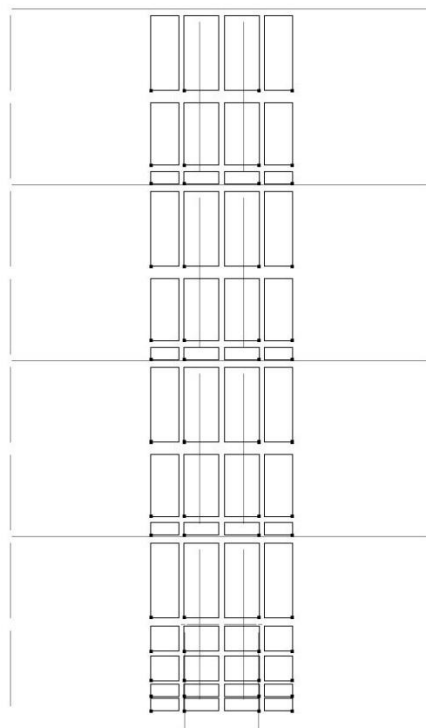


Fig. 7 Elevation View of the Perform 3D Model

SHEAR WALL MODEL

Structural walls were modeled using 4-noded “Shear Wall Elements”⁴ with fiber cross sections. In this implementation, all interconnected planar wall segments at any level are assumed to remain plane when deformed. In the first story, where inelastic actions were expected to concentrate, shear wall elements were meshed so that each element had a height of $2b_w$ (b_w = wall thickness). This value is established from post-earthquake observations of the typical height of spalled regions. For the rest of the building, larger sized elements are used. Due to anticipated low shear demands, an elastic shear material was used for walls, with effective shear stiffness defined as $G_c A_w = 0.4 E_c A_w / 20$ (PEER/ATC-72-1)⁵, in which G_c is shear modulus, E_c is Young’s modulus of concrete (taken as $4700 \bar{f}'_c$, MPa), and A_w is web area. Rocking behavior of wall segments is implemented for wall elements at each floor level. This behavior is achieved by inserting fiber sections at the interfaces having representative compressive behavior but zero tensile strength.

The constitutive material model for concrete is a trilinear idealization of material test results (Figure 8). The stress-strain relationship for confined concrete is implemented using the confinement model for high-strength concrete developed by Razvi & Saatcioglu⁶. Tension resistance of concrete is modeled except for the rocking sections.

Similarly, the reinforcing steel stress-strain relation was a simplified trilinear curve with a descending portion (Figure 9). The ultimate strain of reinforcing steel in tension was limited to 0.05 in consideration of cyclic fatigue (PEER/ATC-72-1)⁵. Behavior in compression was checked according to the ratio s/d_b (s = spacing of transverse reinforcement and d_b = diameter of longitudinal bar) in consideration of longitudinal bar buckling⁷. The adequately small s/d_b ratio is such that reinforcing bars are unlikely to buckle prematurely. The ultimate strain of reinforcing steel under compression nonetheless is limited to 0.02 because of potential buckling at large strains (PEER/ATC-72-1)⁵.

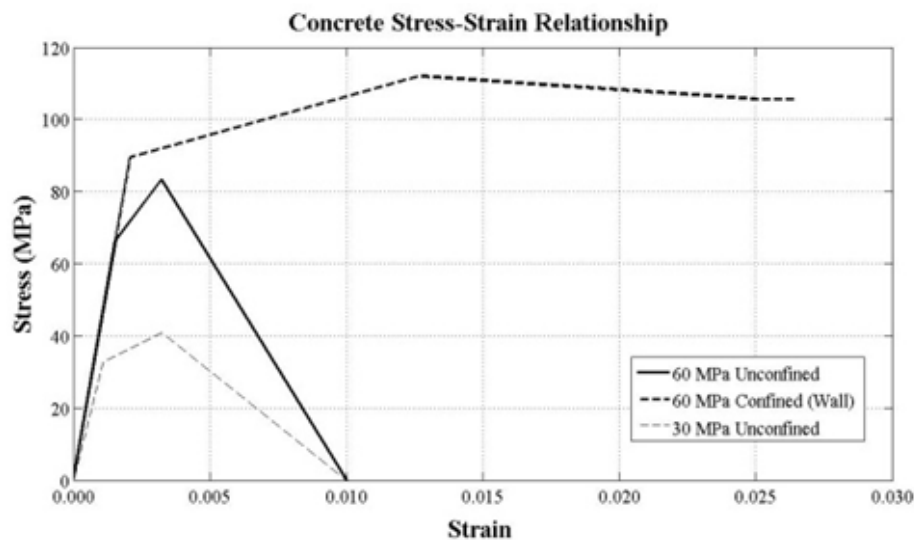


Fig. 8 Concrete Stress-Strain Relation

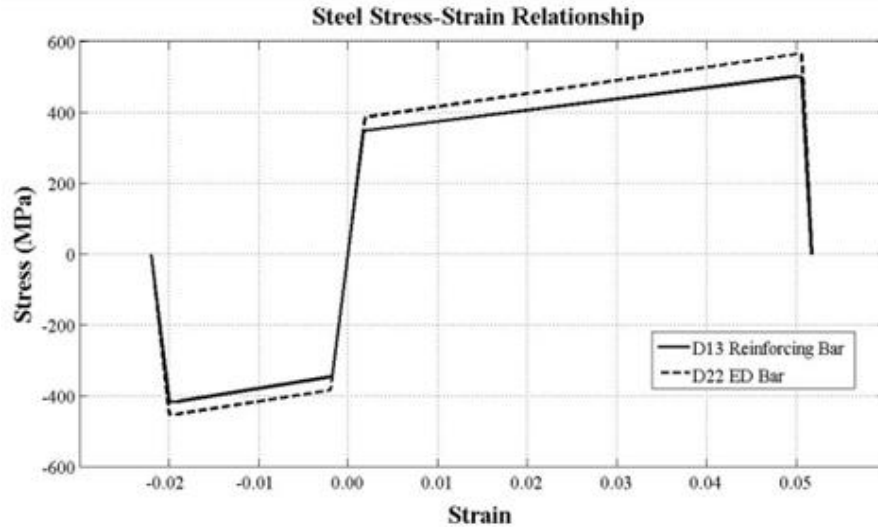


Fig. 9 Reinforcing Bar Stress-Strain Relation

PT tendons and energy dissipation (ED) bars are modelled using truss elements with nonlinear material properties, even though PT tendons stayed in the linear elastic range during the test (Figure 10). Truss elements are connected to shear wall elements through rigid beams extending to locations of tendons and ED bars in the cross section. Lateral displacements of PT tendons are slaved to shear wall elements at each floor level, which is analogous to the effect of the tendon ducts. Truss elements representing the ED bars are modelled along the unbonded length of the bars. Bar slip (strain penetration) effects are considered for modelling of the ED bars. The ED bar trusses are extended below the top of the foundation to mimic the extra elongation caused by slip of the ED bars. Post-tensioning loads on tendons are applied as initial strains concurrently with gravity loads in analysis.

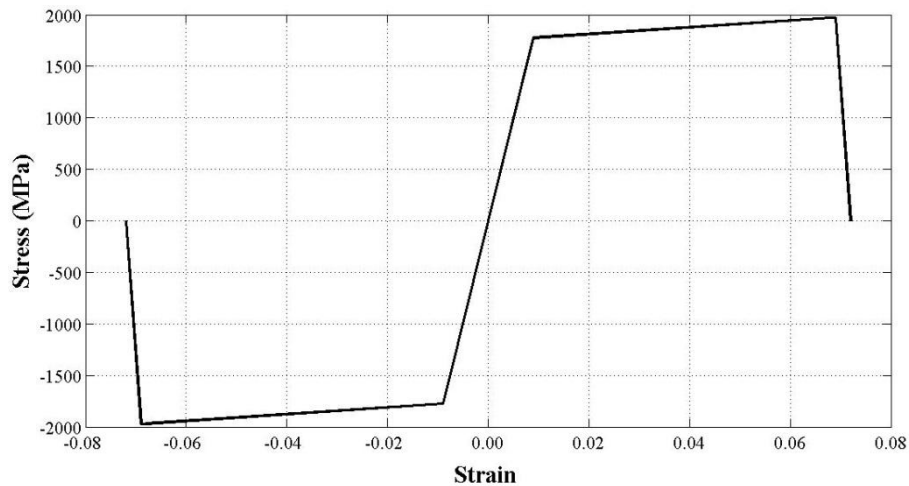


Fig. 10 Post-Tensioned Tendon Stress-Strain Relation

BEAM AND COLUMN MODELS

Beams and columns are modelled using nonlinear beam-column elements with rigid end zones. Nonlinear fiber sections are assigned through the length of elements with distributed plasticity. Similar to the shear wall elements, a simplified trilinear curve with a descending portion is used to model concrete and steel materials. Due to adequate shear design of the members, an elastic shear material was used for beams and columns, with effective shear stiffness defined as $G_c A_w = 0.4 E_c A_w$ (PEER/ATC-72-1)⁵. Similar to rocking sections of wall elements, opening between precast elements is simulated by assigning a “rocking section” to beam element integration points closest to wall and columns). The aforementioned “rocking section” has the same cross section and fiber locations as at other integration points. However, materials assigned to this section are modified to have no tension resistance.

Upper portions of half-precast beams were cast monolithic with the slabs. Beam effective flange widths are calculated using ACI 318⁸ equations. Unlike column elements, for which forces are resisted with fiber sections in both transverse directions, beam elements in Perform 3D use fiber sections only in the major bending axis. Bending stiffness of the minor bending axis is defined with effective bending stiffness $0.5 E_c I_g$, in which I_g is gross section moment of inertia according to the minor bending axis.

Unbonded PT tendons of beams (PG2 & PG3) are modelled with parallel truss elements with nonlinear material properties. Their vertical displacements through beams and walls are slaved to parallel elements similar to modelling of ducts for walls. Similar to PT tendons of walls, post-tensioning loads on tendons are applied as initial strains. In contrast, bonded PT rods of columns (PC1) are included in the fiber cross-section. Post-tensioning loads on columns are approximated by applied point loads (in the same direction with gravity).

MISCELLANEOUS NOTES ON THE NUMERICAL MODEL

Rayleigh damping is used for nonlinear response history analysis, with parameters set to produce 2 percent damping at periods $T_1/8$ and $1.25T_1$, where $T_1 = 0.29$ seconds. All analyses were in the Y direction; therefore, X-direction displacements of all nodes are restrained. After the application of gravity and prestressing loads, the model is excited with 25%, 50%, and 100% Kobe motions, respectively.

COMPARISON OF SIMULATION AND TEST RESULTS

Prior to application of earthquake motions, the test building was excited with white noise. Fundamental periods of the building were 0.29 s in the Y direction and 0.45 s in the X direction. Modal analysis of the numerical model resulted a fundamental period of 0.29 s in the Y direction.

Base shear versus roof drift ratio responses of the numerical model and test specimen under 25%, 50%, 100% Kobe excitations are shown in Figures 11, 13, and 15. Comparisons of roof drift ratio versus time responses of numerical model and test specimen are shown in Figures 12, 14, and 16. Flag-shaped hysteresis typical of unbonded post-tensioned concrete is apparent. The numerical model and test results are in very good agreement for important engineering parameters, such as stiffness, maximum base shear, and maximum roof drift. For

all excitations, energy dissipated during the earthquake (area inside the hysteresis curve) is estimated with a good accuracy.

Although estimated maximum roof drift ratios are very close to the test results, phase shifts in roof drift ratio versus time are significant for some parts of the response. The roof drift ratio response history estimate for the 25% Kobe motion shifts out-of-phase after 19 s. The vibration period of the test specimen is increasing after 19 s, but the numerical model does not identify this increase in period.

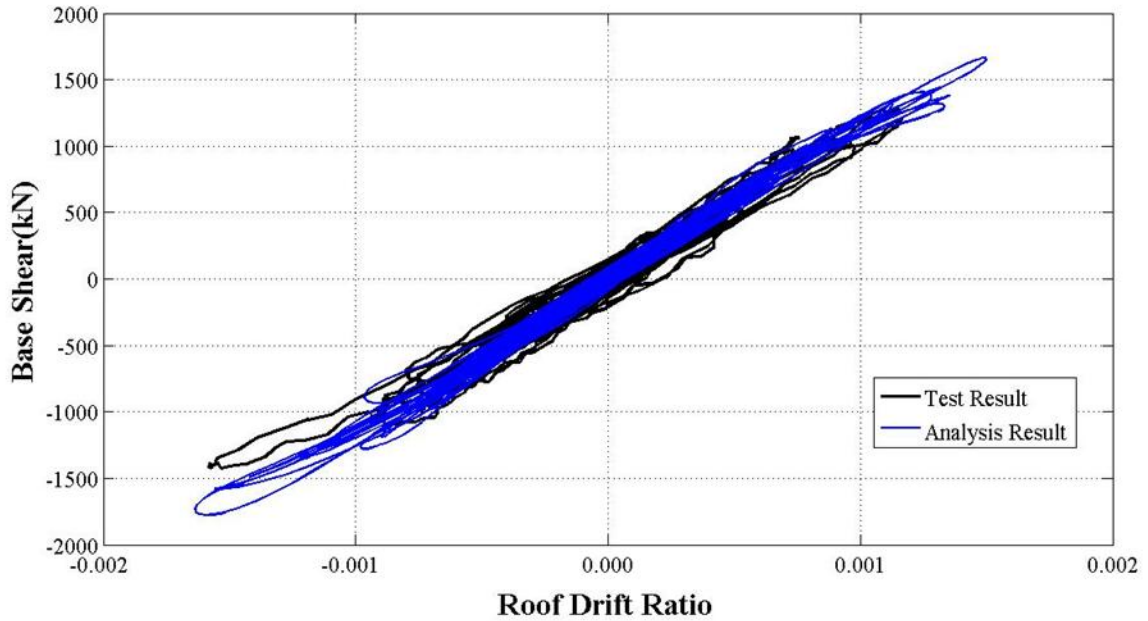


Fig. 11 Base Shear-Roof Drift Ratio Comparison of Results of 25% Kobe Motion

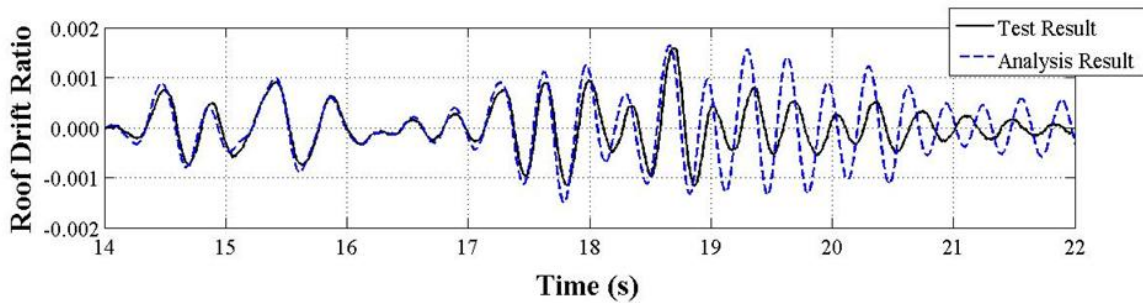


Fig. 12 Roof Drift Ratio-Time Comparison of Results of 25% Kobe Motion

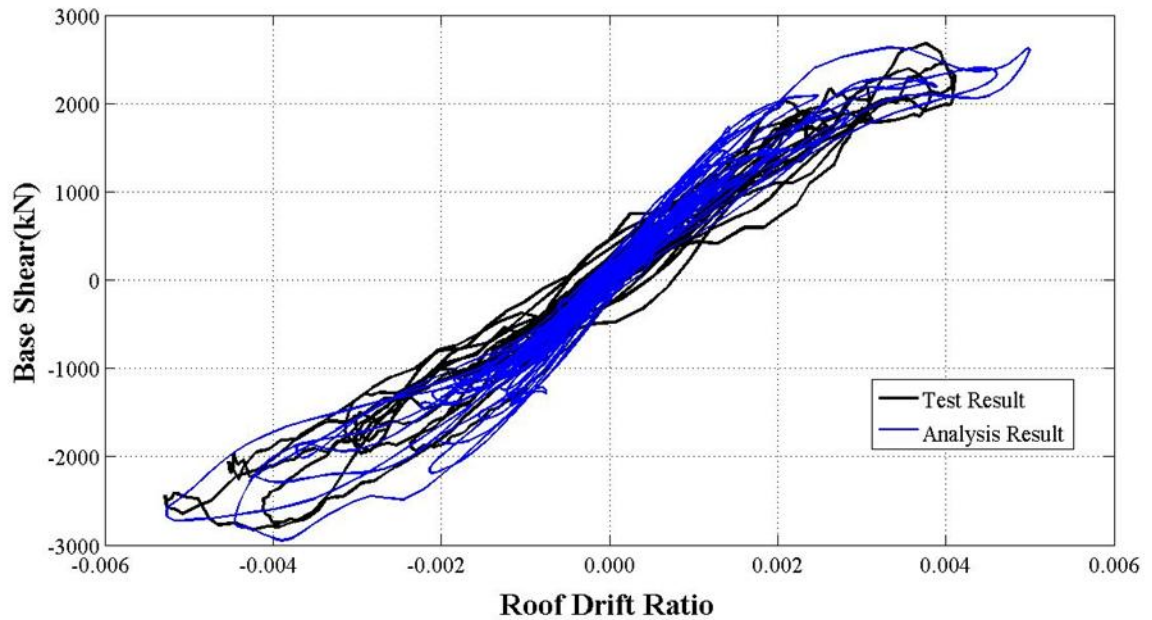


Fig. 13 Base Shear-Roof Drift Ratio Comparison of Results of 50% Kobe Motion

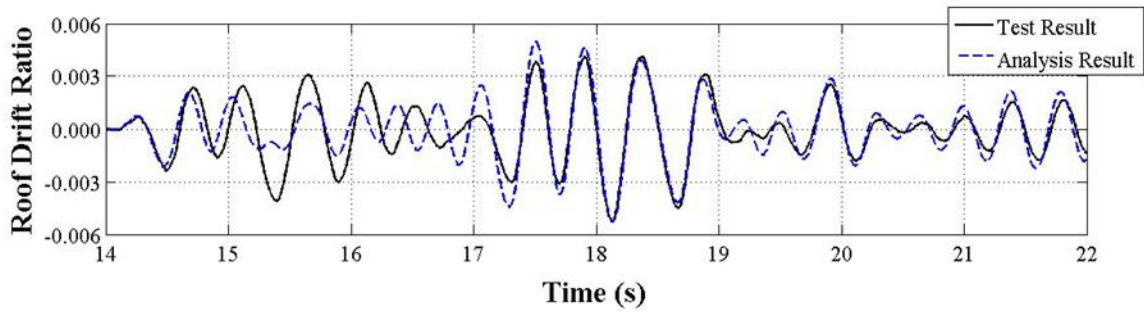


Fig. 14 Roof Drift Ratio-Time Comparison of Results of 50% Kobe Motion

The calculated roof drift ratio history for the 100% motion also does not estimate the increase in vibration period after 21 s. Measured and calculated response decay near the end of the test match fairly closely for the 50% and 100% Kobe motion, suggesting the damping is modeled reasonably. For the 25% motion response, calculated response damps out more slowly than the test results.

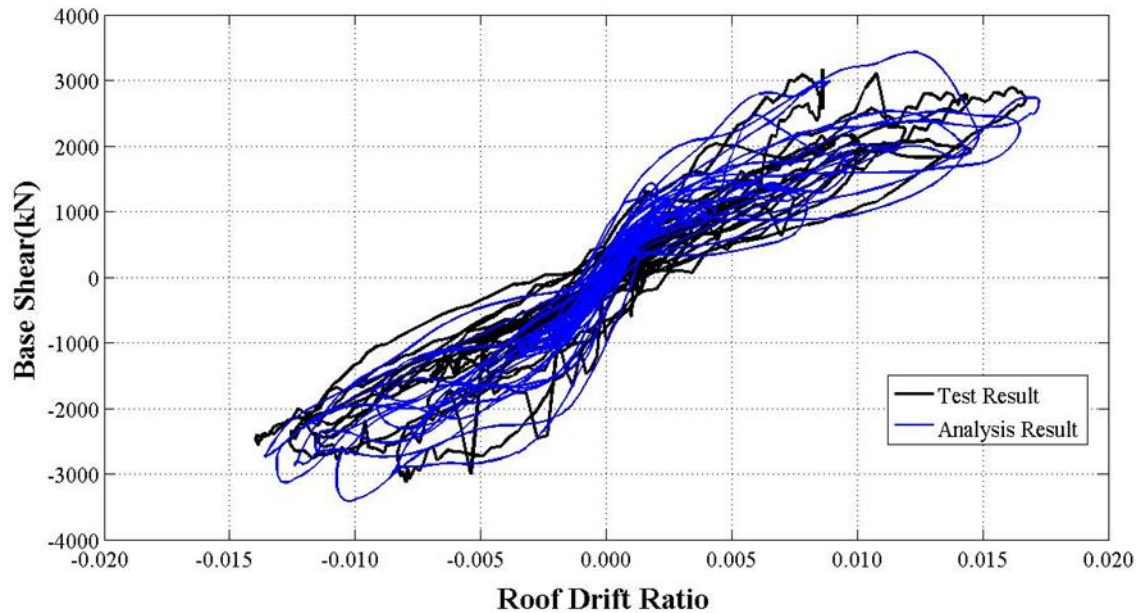


Fig. 15 Base Shear-Roof Drift Ratio Comparison of Results of 100% Kobe Motion

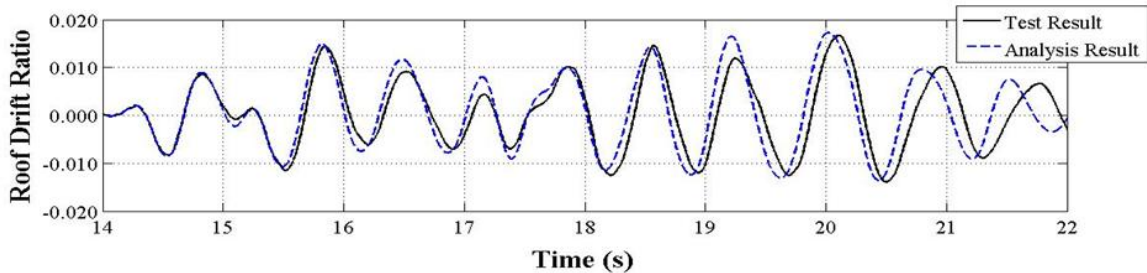


Fig. 16 Roof Drift Ratio-Time Comparison of Results of 100% Kobe Motion

CONCLUSIONS

A three-dimensional earthquake simulation test on a full-scale, four-story, prestressed concrete building is conducted using the E-Defense shaking table facility. The seismic force-resisting system of the test building comprised two post-tensioned (PT) frames in one direction and two unbonded PT precast walls in the other direction. The test building was subjected to several earthquake ground motions, ranging from serviceability level to near collapse. The wall direction (Y direction) of the building is modeled using the computer program Perform 3D, with emphasis on a model that would be practical for design-office implementation. This model is subjected to several base motions to explore the accuracy of the numerical model.

Important engineering parameters such as fundamental vibration period, stiffness, hysteresis shape, maximum base shear, and maximum roof drifts are adequately simulated using the numerical model. There are, however, some discrepancies in variation of these responses with time. These results indicate that, while further improvements may be

desirable, the selected modelling approach is capable of producing seismic response estimates of sufficient accuracy to be used for detailed design of unbonded post-tensioned, precast structural wall systems.

ACKNOWLEDGEMENTS

The writers acknowledge the funding provided to participate in the tests by the U.S. National Science Foundation. Funding for this study provided by Pacific Earthquake Engineering Research (PEER) Center and Precast/Prestressed Concrete Institute (PCI) Daniel P. Jenny Fellowship is gratefully acknowledged. The writers also thank Computers & Structures, Inc. (CSI) for providing the computer software used for this study. Lead participation of T. Nagae, T. Matsumori, H. Shiohara, T. Kabeyasawa, S. Kono, K. Tahara, and M. Nishiyama from Japan side and J. Wallace, W. Ghannoum, and R. Sause from the U.S side is gratefully acknowledged.

REFERENCES

1. ACI ITG-5.2-09 (2009), "Requirements for Design of Unbonded Post-Tensioned Precast Shear Wall Satisfying ACI ITG-5.1 (ACI ITG-5.2-09) and Commentary," American Concrete Institute, Farmington Hills, Michigan.
2. Priestley, M.J.N. (1991), "Overview of the PRESSS Research Program," *PCI Journal*, Precast/Prestressed Concrete Institute, 41(2), 22-40.
3. Nagae, T. A., Tahara, K., Matsumori, T., Shiohara, H., Kabeyasawa, T., Kono, S., Nishiyama, M., Wallace, J., Ghannoum, W., Moehle, J.P., Sause, R., Keller, W., and Tuna, Z. (2011), "Design and Instrumentation of the 2010 E-Defense Four-Story Reinforced Concrete and Post-Tensioned Concrete Buildings," *Technical Report 2011/104*, Pacific Earthquake Engineering Research Center, University of California, Berkeley.
4. Computers and Structures, Incorporated (CSI), "Perform 3D, Nonlinear Analysis and Performance Assessment for 3D Structures,"
5. PEER/ATC-72-1 (2010), "Modeling and Acceptance Criteria for Seismic Design and Analysis of Tall Buildings," Applied Technology Council, Redwood City, CA.
6. Razvi, S., and Saatcioglu, M. (1999), "Confinement Model for High-Strength Concrete," *Journal of Structural Engineering*, American Society of Civil Engineers, 125(3), 281-289.
7. Monti, G., and Nuti, C. (1992), "Nonlinear Cyclic Behavior of Reinforcing Bars Including Buckling," *Journal of Structural Engineering*, American Society of Civil Engineers, 118(12), 3268-3284.
8. ACI 318-08 (2008), "Building Code Requirements for Structural Concrete (ACI 318-08) and Commentary," American Concrete Institute, Farmington Hills, Michigan.
9. Tanyeri, A.C., Moehle, J.P., Nagae T. (2012), "Seismic Performance and Modelling of Post-Tensioned, Precast Concrete Shear Walls", *15th World Conference on Earthquake Engineering*, Lisbon 2012